

Surface Bi-Directional Reflectance Properties Over the ARM SGP Area from Satellite Multi-Platform Observations

*Y. Luo, A. P. Trishchenko, and R. Latifovic
Canada Centre for Remote Sensing
Natural Resources Canada
Ottawa, Ontario, Canada*

*Z. Li
Earth System Science Interdisciplinary Center
University of Maryland
College Park, Maryland*

Introduction

Surface albedo is an important parameter in atmospheric radiation research. Good knowledge of surface bi-directional reflectance distribution function (BRDF) is essential in order to obtain the hemispheric reflectance (albedo) using data from satellite systems, which only view the ground at particular angles. Linear kernel-driven BRDF models have been commonly used for simple operational implementation of inversion procedure for derivation of model parameters. As an alternative to pixel-based approach in deriving BRDF parameters that uses all clear-sky pixel identified at particular point, a landcover-based approach is followed here assuming similarity in BRDF for the same landcover type in similar conditions. This approach is particularly suitable for the agriculture dominant area of the South Great Plain (SGP) where there are a limited number of cover types and within each type surface condition is fairly uniform unlike the majority of natural scenes. The approach can overcome a major limitation of pixel-based approach that is much more demanding on computational resources, and low number of observations for each particular point may impact adversely on the quality of BRDF parameters. Landcover-based approach provides much better sampling in terms of number of observations, requires less computational resources, may be implemented for shorter time intervals; however, may not always capture some spatial differences in the BRDF behavior.

In this study, we use data available from POLarization and Directionality of the Earth's Reflectance (POLDER) instrument to evaluate the performance of several BRDF models for cropland mosaic in the SGP area. Then data from several medium-resolution satellite sensors, such as multi-angle imaging spectroradiometer (MISR), moderate resolution imaging spectroradiometer (MODIS), vegetation (VGT) sensor and advanced very high resolution radiometer (AVHRR), are used to investigate variability and dynamics of the BRDF shape in various spectral bands. The data from high-resolution sensor like Landsat-7 is also used to identify the surface conditions in details. An approach for BRDF reconstruction based on the landcover type is applied to generate surface spectral albedo/BRDF datasets

using clear-sky multiday composites. Some results of comparison between these models and observed seasonal dynamics of BRDF properties are presented.

BRDF Models

BRDF is a measure of surface anisotropic reflectance, which is dependent upon both solar and viewing geometries. A linear BRDF model is typically expressed as a sum of several theoretically constructed kernel functions $f_i(\theta_s, \theta_v, \phi)$; among them θ_s , θ_v and ϕ are solar zenith angle, viewing zenith angle and relative azimuth angle between the Sun and viewer. The model of Roujean (Roujean et al. 1992) and RossThick-LiSparse (Wanner et al. 1997) are all such kind of model with 3 kernels as follows

$$\rho_\lambda(\theta_s, \theta_v, \phi) = \sum_{i=0}^2 a_i f_i(\theta_s, \theta_v, \phi) \quad (1)$$

a_0 , a_1 and a_2 are coefficients of the kernels and represent isotropic, volumetric and geometric reflectance, respectively.

The modified Rahman's model (Rahman et al. 1993; Martonchik 1997) is non-linear but can be converted into linear form by taking the logarithm of the function

$$\rho_\lambda(\theta_s, \theta_v, \phi) = a_0 P(a_1, \xi) [1 + R(\xi)] \frac{\cos^{a_2-1} \theta_s \cos^{a_2-1} \theta_v}{(\cos \theta_s + \cos \theta_v)^{1-a_2}} \quad (2)$$

ξ is the reflective angle (angle between the observer and the Sun relative to the target), P is a phase function, and $(1 + R)$ is a factor to account for the hot spot effect.

A modified version of the Roujean's model developed at Canada Centre for Remote Sensing (Chen and Cihlar 1997) is

$$\rho_\lambda(\theta_s, \theta_v, \phi) = \sum_{i=0}^2 a_i f_i(\theta_s, \theta_v, \phi) (1 + a_3 e^{-a_4 \xi / \pi}) \quad (3)$$

The first 3 parameters are the same as in the Roujean's model, but a_3 and a_4 are used for the hot spot effect. The process of model inversion is to determine its parameters through optimum fitting of the observed dataset.

To evaluate performance of above BRDF models we used multiangular observations available from POLDER instrument (http://smc.cnes.fr/POLDER/A_produits_scie.htm). The fitted parameters and quality of fitting are presented in Table 1, and the reflectances and model results are shown in Figure 1 for cropland mosaic. The Roujean's, Ross-Li and Rahman's have similar performance and the modified

Table 1. Model parameters from different BRDF models.

| BRDF Model | | a_0 | a_1 | a_2 | a_3 | a_4 | Errors (%) |
|--------------------|------|--------|--------|--------|--------|--------|------------|
| Roujean's | Blue | 0.0702 | 0.0314 | 0.0159 | -- | -- | 11.02 |
| | Red | 0.1519 | 0.2158 | 0.0392 | -- | -- | 3.75 |
| | NIR | 0.2513 | 0.3280 | 0.0627 | -- | -- | 2.82 |
| RossThick-LiSparse | Blue | 0.0679 | 0.0077 | 0.0142 | -- | -- | 11.11 |
| | Red | 0.1468 | 0.0384 | 0.0354 | -- | -- | 3.96 |
| | NIR | 0.2435 | 0.0527 | 0.0573 | -- | -- | 2.93 |
| Modified Roujean's | Blue | 0.0476 | 0.0102 | 0.0049 | 0.9010 | 7.8139 | 10.13 |
| | Red | 0.1248 | 0.1519 | 0.0127 | 0.4765 | 8.6997 | 2.43 |
| | NIR | 0.2153 | 0.2451 | 0.0273 | 0.3752 | 8.8474 | 1.68 |
| Rahman | Blue | 0.0575 | 0.5947 | 1.2861 | -- | -- | 11.54 |
| | Red | 0.1473 | 0.8730 | 1.4453 | -- | -- | 5.24 |
| | NIR | 0.2460 | 0.8188 | 1.4266 | -- | -- | 4.33% |

Roujean's has slightly better accuracy, which is reasonable to expect given that it includes two more fitting parameters. The performance of various models has been investigated in detail by some other researchers. For example, Privette et al show that among those 3-parameter models and for data with limited angular distributions the Ross-Li and Rahman's model have a better performance (e.g., Privette et al. 1997). In the following BRDF retrievals we use Ross-Li model.

BRDF Retrievals in Landcover-Based Approach

Landcover map. We present in this section some results of BRDF retrievals using landcover-based approach. To this end, we used an IGBP landcover map, which is from the Land Processes Distributed Active Archive Center (http://edcdaac.usgs.gov/glcc/globdoc1_2.html). There are about 12 landcover types in the ARM SGP area, as shown in Figure 2. The Central Facility (CF) is marked with a cross symbol. The basic idea is to use multi-day composite surface reflectance datasets for BRDF fitting. Instead of pixel-based data collection and model inversion, landcover-based fitting strategy is employed to have observations corresponding various observational geometrical conditions (Cihlar et al. 2002, Trishchenko et al. 2002a). The total pixel number for area like in Figure 2 is 1121×897 when the pixel resolution is $1 \times 1 \text{ km}^2$ on the ground. Because there are large amounts of pixels for some dominated land types, such as grass, cropland and forest, data from same landcover are categorized into data bins according to their geometric information that is solar zenith, view zenith and relative azimuth angle. Data in each bin are statistically averaged before going to fitting process. To reduce scattering and derive more representative BRDF shape for a certain pure landcover type we collected pixels for a

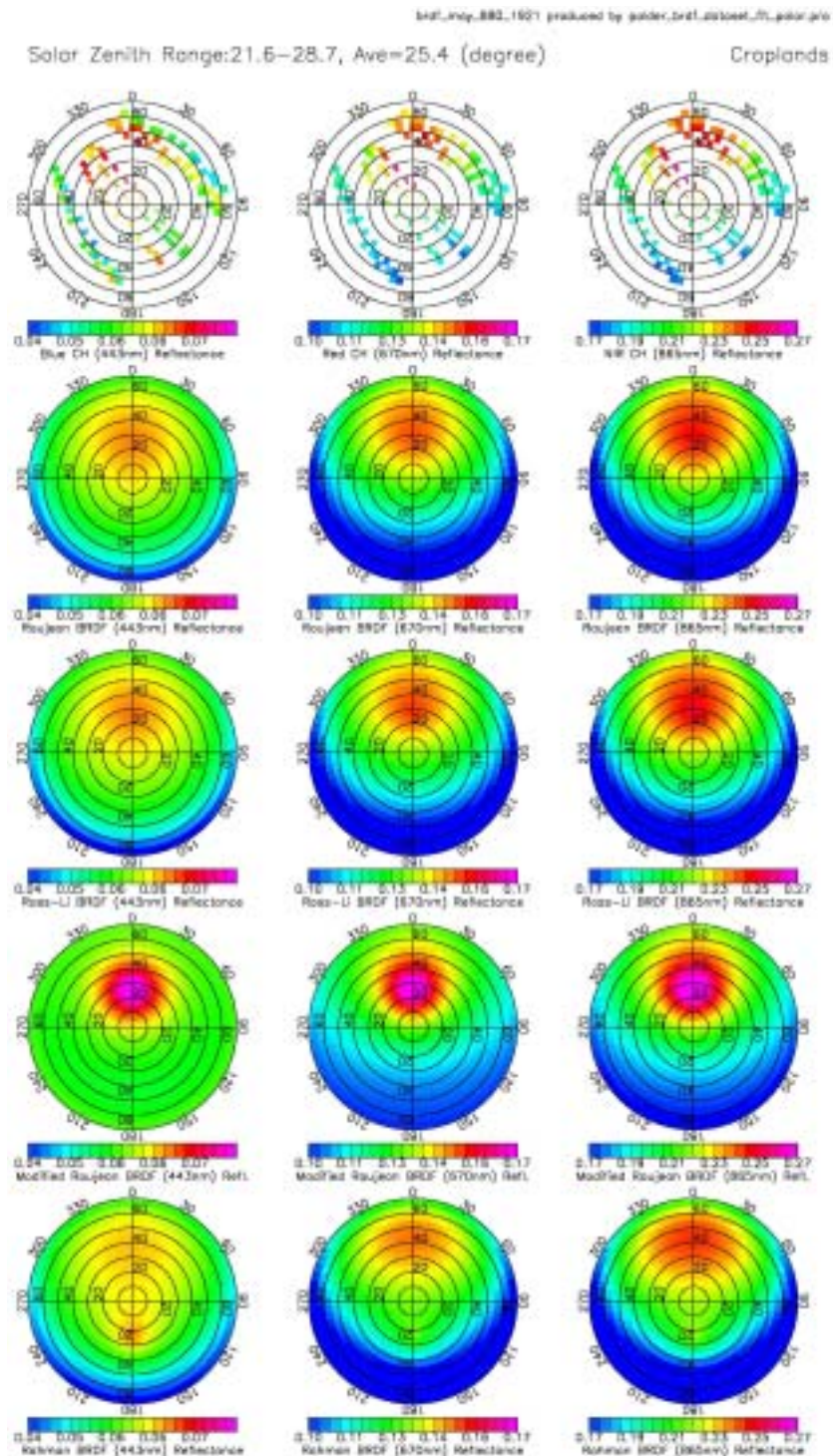


Figure 1. Polar plots of surface reflectance at 3 bands (blue, red and NIR) from croplands in ARM SGP area in May. From the top to the bottom are observed by POLDER, and model results from Roujean's, Ross-L, modified Roujean's and Rahman's BRDF models. The radius represents the viewing zenith angle, the polar angle the relative azimuth between the Sun and viewer. The model parameters are listed in Table 1.

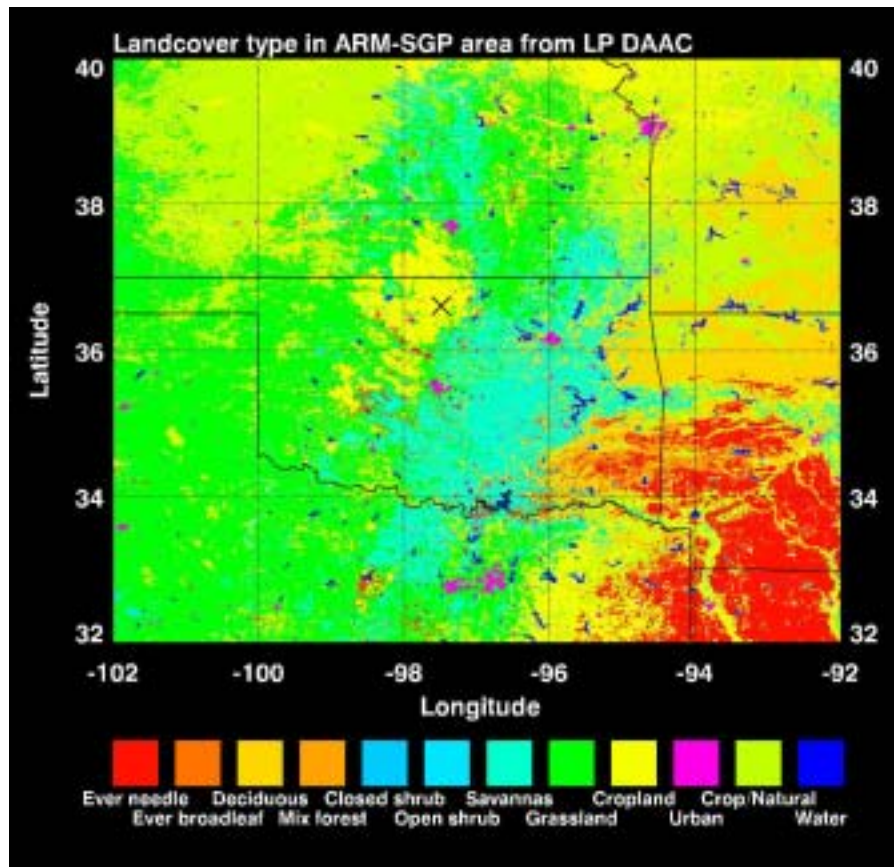


Figure 2. The distribution of the land-cover types around the ARM SGP area (IGBP classification). There are total 12 land types identified in this area. The cross-symbol at the center indicates the location of the ARM central facility.

certain landcover type only when all other pixels surrounding the selected pixel have the same land type. All pixels with bad quality or cloud contamination are eliminated according to their flag dataset.

Variability within landcover class. To give an idea about variability of surface properties for the same landcover class, we selected a $2 \times 2 \text{ km}^2$ cropland area in the vicinity of CF. This area is depicted on Landsat-image taken on March 9, 2002 (Figure 3). The cropland color shown in Figure 3 varies from dark green to light brown, which corresponds to different vegetation conditions within each pixel area.

Figure 4 shows also variability of the reflectances within each MISR pixel. Since the vegetation conditions can be described by Normalized Difference Vegetation Index (NDVI), we also suggest including this parameter as an independent variable (see Figure 4).

BRDF fitting for large area. In our final scheme we use 3 angles and NDVI as independent parameters. We divide data into different groups by NDVI levels, and do fitting separately for each group. Figure 5 shows the 4-band reflectances (black squares) and Ross-Li modeling values for cropland in the ARM-SGP area from VGT observation. Each black square comes from a statistical result in each data bin. Figure 6 shows the same but 7 bands from MODIS.



Figure 3. View of the ARM SGP area from Landsat-7 on March 9, 2002. The cropland sampling square corresponds roughly to a 2 x 2 km² area that is by 4 pixels in MISR scan in Figure 4.

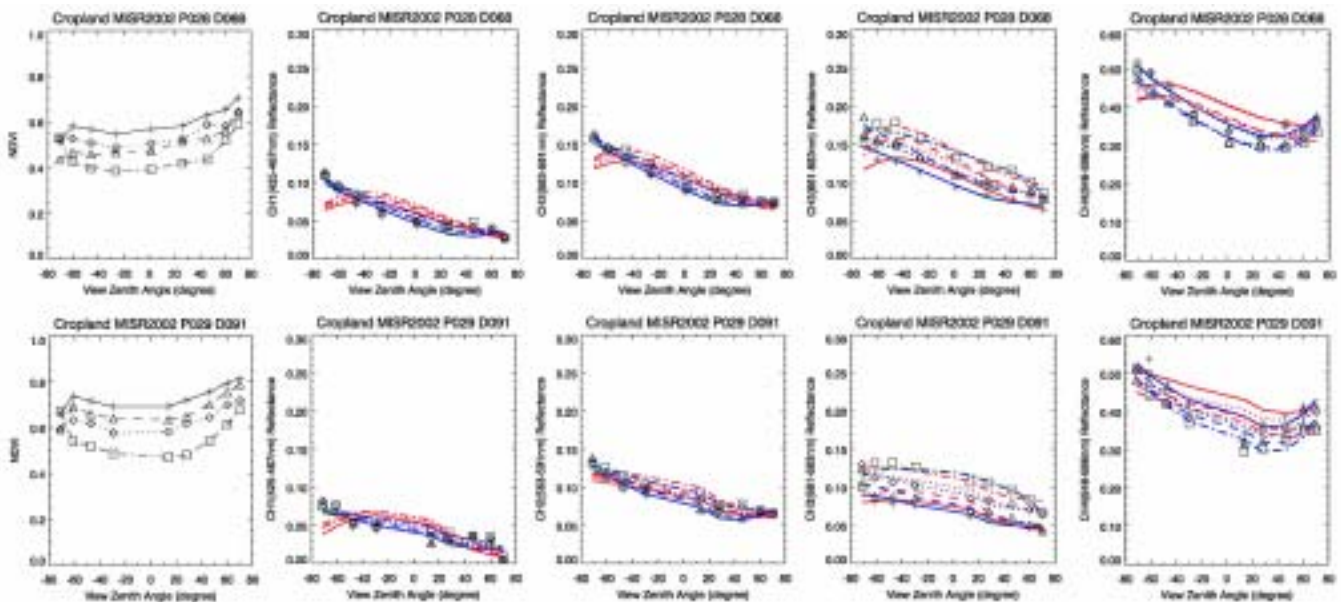


Figure 4. The NDVI and surface reflectances of the cropland sampling square as in Figure 4 observed by MISR on the same day, March 9, 2002, (upper) and 3 weeks later, April 1, 2002 (lower). A 2 x 2 km² area correspond to 4 pixels in MISR scan which are denoted by symbols of diamond, cross, triangle and square, in an order shown in Figure 3. Due to different vegetation densities within this square the 4 pixels have significantly different NDVI and reflectance features. They also change after 3 weeks. The color lines are BRDF model fittings, the red is model of Rahman, the blue and green are of Ross-Li and Roujean, respectively.

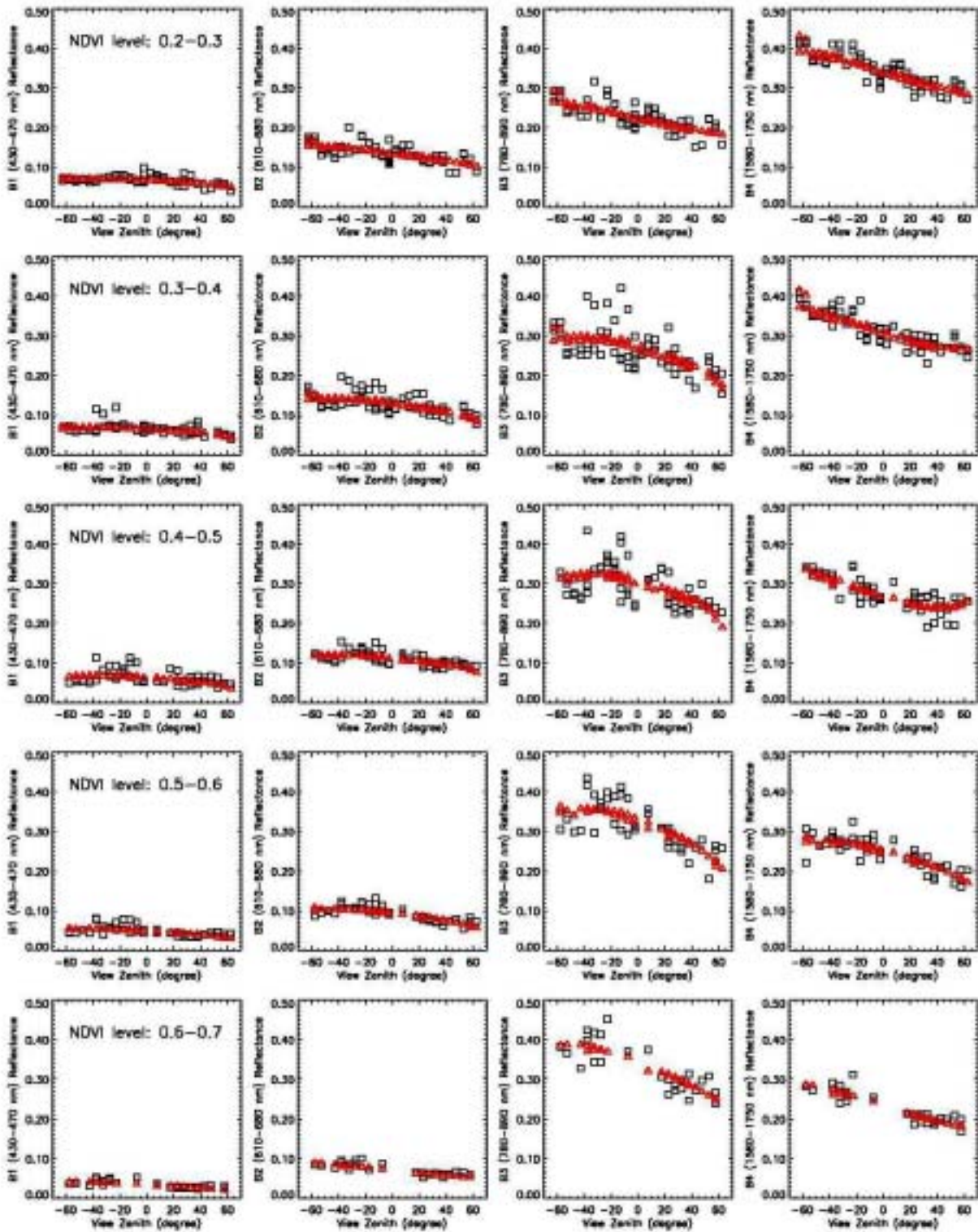


Figure 5. VGT 4-band (from left to right: 430-470, 610-680, 780-890, and 1580-1750 nm) cropland reflectances (black square) against view zenith angles at different NDVI levels in April 2002. The red triangles are Ross-Li BRDF fitted values at the same geometries.

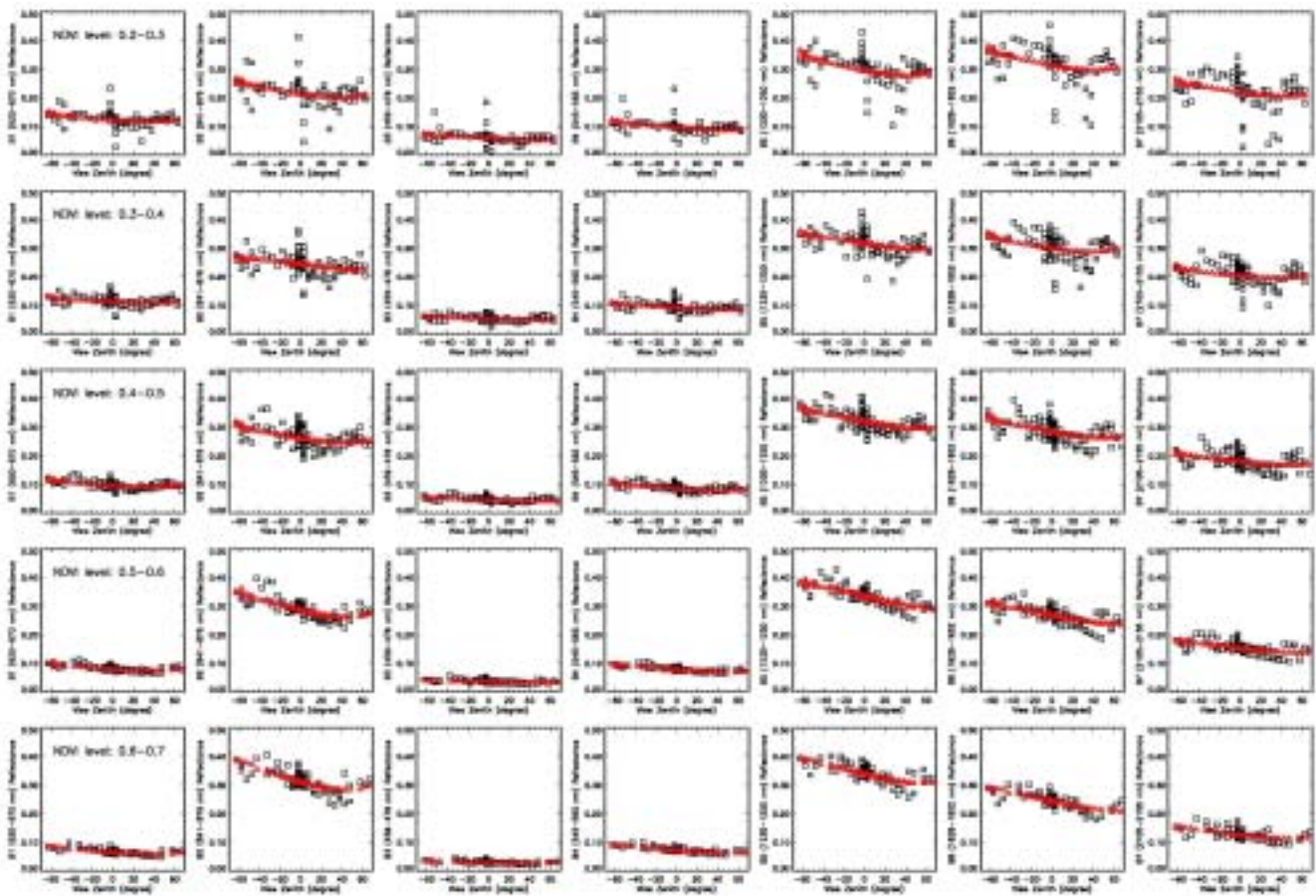


Figure 6. Same as Figure 6 but for MODIS 7 bands (from left to right: 620-670, 841-876, 459-479, 545-565, 1230-1250, 1628-1652, and 2105-2155 nm).

We can apply the above BRDF model and methodology to data from multiple-satellite observations. An example is displayed in Figure 7 for this application to MODIS 8-day (MOD09a1) and VGT data, and comparison with results from albedo products of MODIS (MOD43B3) (Schaaf et al. 2002) and MISR (MISR L2) (Diner et al. 1999).

Another application of the BRDF model is to obtain normalized reflectances, which can indicate the seasonal variations. Figure 8 shows the red and NIR band nadir reflectance for grassland and cropland from VGT observation in year 2000.

Summary

Several BRDF models are evaluated with multi-sensor datasets. All models show reasonable fitting accuracy. The fitting quality depends greatly on the geometric coverage of the dataset, especially for retrieving the hot-spot effect.

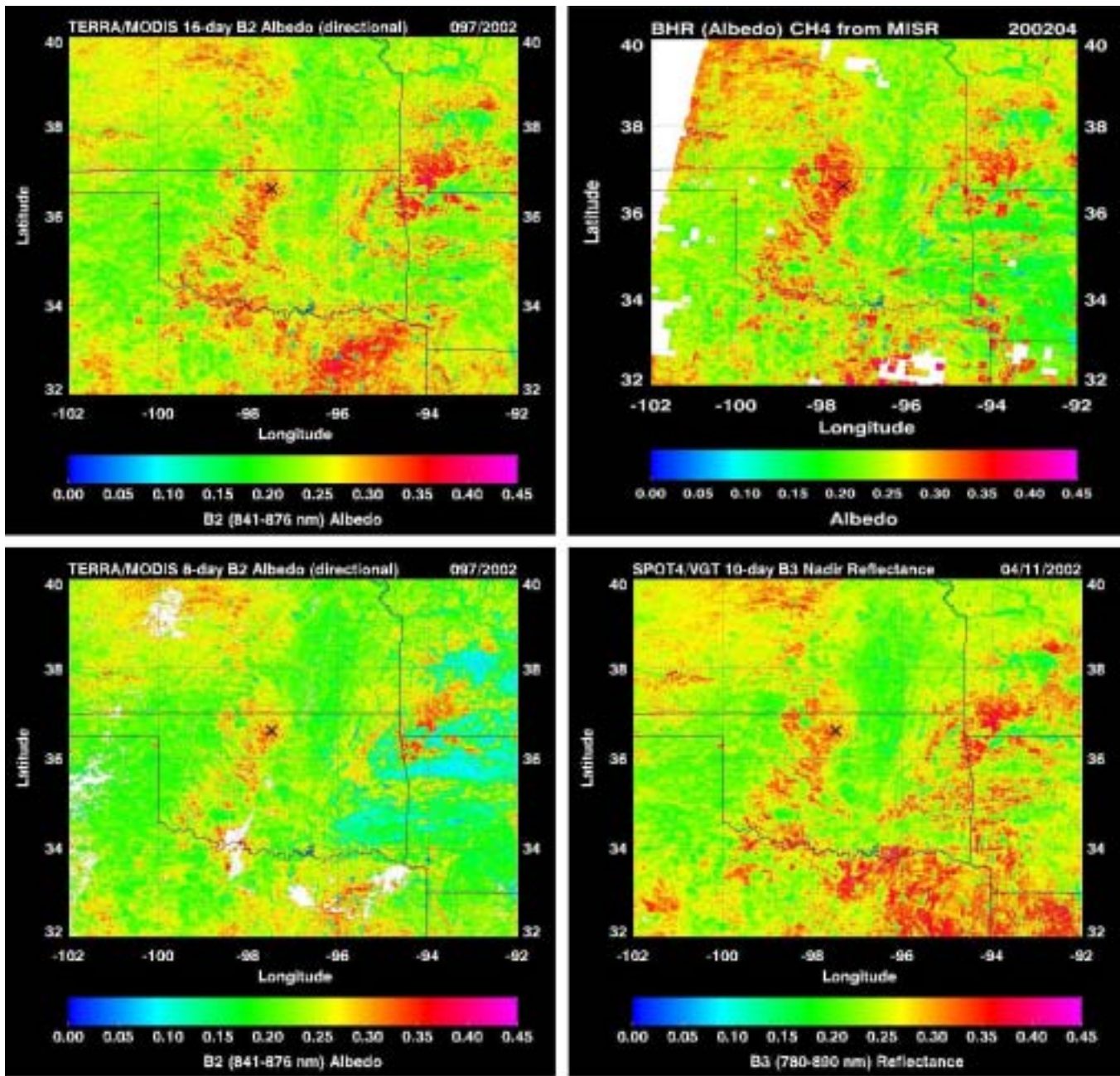


Figure 7. The NIR band albedo or reflectance around the ARM-SGP area from several sensors during the same period, i.e., the middle of April, 2002. The bandwidths are 841-876, 846-886, 780-890 nm and for MODIS, MISR and VGT, respectively. The cross-symbol near the map centre indicates the location of the ARM central facility. The upper two are MODIS and MISR albedos from MOD43B3 and MISR L2 land surface products. The lower two are MODIS 8-day albedo and VGT nadir reflectance (local noon), which are generated through the landcover based process. The white color in images indicates data gaps.

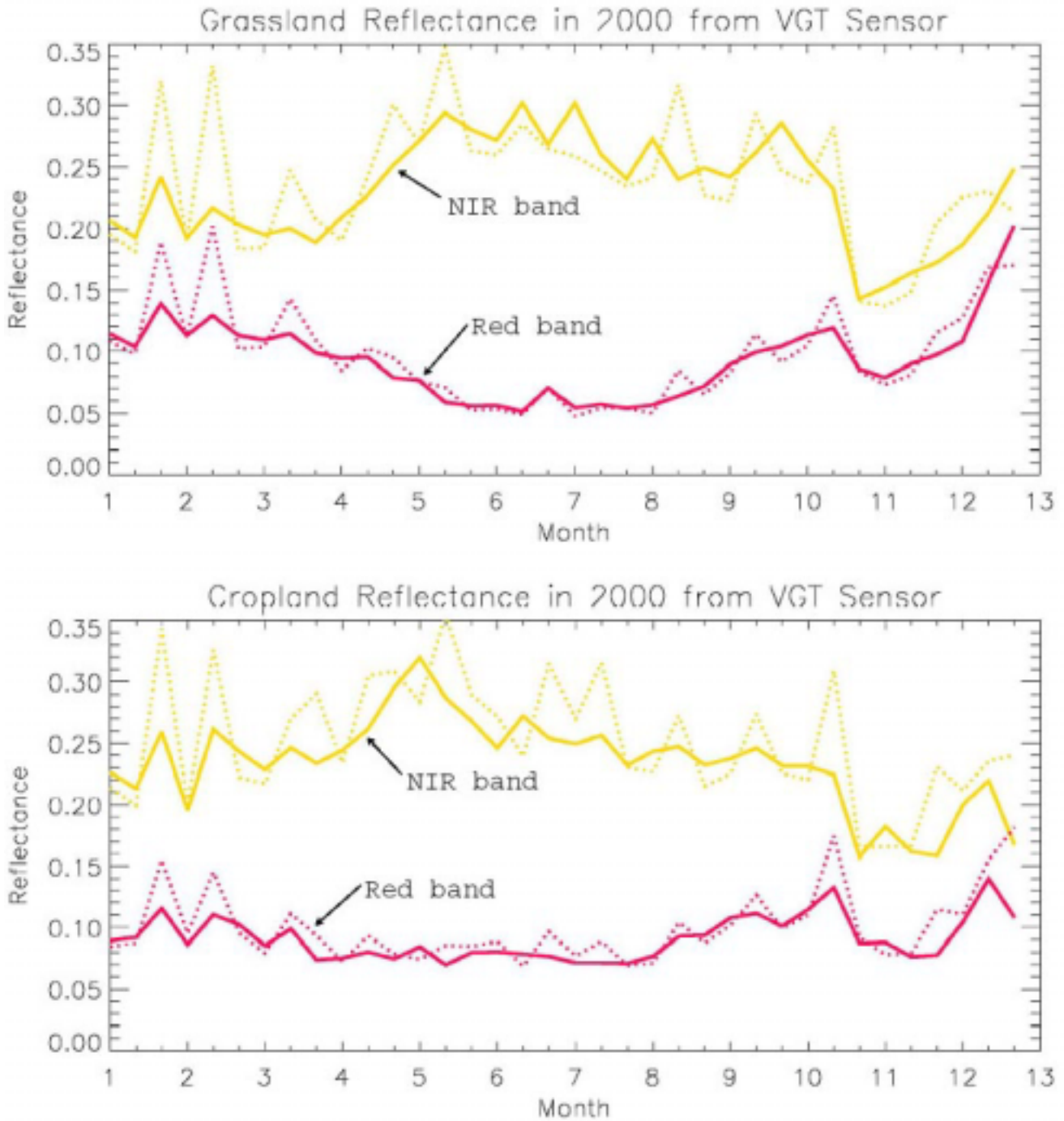


Figure 8. The seasonal variation of grass- and crop-land reflectances from VGT. The solid lines are BRDF corrected (i.e., nadir view) and the dashed are before correction.

Landcover-type based approach is implemented to process data and perform the BRDF model inversion. The data are categorized into small predefined geometric and NDVI bins and processed statistically in each data bin. This will eliminate the observation outliers and increase the accuracy.

Comparison with other products (MODIS and MISR) shows encouraging results. Further validation and comparison among different sensors, and improvement are in process.

Based on the above studies, we are generating a surface albedo datasets that include data from multiple platforms to obtain more accurate BRDF properties and surface albedo properties (Trishchenko et al. 2002 a,b).

Acknowledgment

This research was supported by the U.S. Department of Energy Atmospheric Radiation Measurement (ARM) Program, Grant No. DE-FG02-02ER63351.

Corresponding Author

Y. Luo, Yi.Luo@nrcan.gc.ca, (613) 992-8796

References

Chen, J., and J. Cihlar, 1997: A hot spot function in a simple bidirectional reflectance model for satellite applications. *J. Geophys. Res.*, **102**(25) 907–913.

Cihlar, J., J. Chen, Z. Li, R. Latifovic, G. Fedosejev, M. Adair, W. Park, R. Fraser, A. Trishchenko, B. Guindon, D. Stanley, and D. Morse, 2002: GeoComp-n, an advanced system for the processing of coarse and medium resolution satellite data. Part 2: Biophysical Products for Northern Ecosystems. *Can. J. Remote Sens.*, **28**, 21-44.

Diner, D. J., J. V. Martonchik, C. Borel, S. A. W. Gerstl, H. R. Gordon, Y. Knyazikhin, R. Myneni, B. Pinty, and M. Verstraete, 1999. *MISR Level 2 Surface Retrieval*. Report of JPL D-11401. (http://eospsso.gsfc.nasa.gov/eos_homepage/for_scientists/atbd/docs/MISR/atbd-misr-10.pdf)

Martonchik, J. V., 1997: Determination of aerosol optical depth and land surface directional reflectances using multi-angle imagery. *J. Geophys. Res.*, **102**(17) 15-22.

Privette, J. L., T. F. Eck, and D. W. Deering, 1997: Estimating spectral albedo and nadir reflectance through inversion of simple BRDF models with AVHRR/MODIS-like data. *J. Geophys. Res.*, **102**(29) 529-542.

Rahman, H., B. Pinty, and M. Verstraete, 1993: Coupled surface atmosphere reflectance (CSAR) model, 2, Semiempirical surface model usable with NOAA advanced very high resolution radiometer data. *J. Geophys. Res.*, **98**(20) 791-801.

Schaaf, C. B., F. Gao, and A. H. Strahler, 2002: First operational BRDF, albedo nadir reflectance products from MODIS. *Remote Sens. Environ.*, **83**(135) 148.

Roujean, J. L., M. Leroy, A. Podaire, and P. Y. Deschamps, 1992: Evidence of surface reflectance bidirectional effects from a NOAA/AVHRR multitemporal dataset. *Int. J. Remote Sens.*, **13**, 685–698.

Trishchenko, A. P., Y. Luo, R. Latifovic, W. Park, J. Cihlar, and Z. Li, 2002a: Mapping surface reflective properties over the ARM SGP CART area by combining multi-platform observational datasets. *Proc. 11th AMS Conference on Atmospheric Radiation*, pp.82-85.

Trishchenko, A. P., Y. Luo, R. Latifovic, W. Park, J. Cihlar, B. Hwang, Z. Li, and M. Cribb, 2002b: Towards development of a synthesized database of spatial and temporal surface spectral reflectivity over the ARM SGP CART area. In *Proceedings of the Twelfth Atmospheric Radiation Measurement (ARM) Science Team Meeting*, ARM-CONF-2002. U.S. Department of Energy, Washington, D.C. Available URL: [http://www.arm.gov/docs/documents/technical/conf_0204/trishchenko\(3\)-ap.pdf](http://www.arm.gov/docs/documents/technical/conf_0204/trishchenko(3)-ap.pdf)

Wanner, W., A. H. Strahler, B. Hu, P. Lewis, J.-P. Muller, X. Li, C. L. Barker Schaaf, and M. J. Barnsley, 1997: Global retrieval of bidirectional reflectance and albedo over land from EOS MODIS and MISR data: Theory and Algorithm. *J. Geophys. Res.*, **102**(17), 143-161.